Catalase Protects Cardiomyocyte Function in Models of Type 1 and Type 2 Diabetes

Gang Ye,[1] Naira S. Metreveli,[1] Rajakumar V. Donthi,[1] Shen Xia,[1] Ming Xu,[1] Edward C. Carlson,[2] and Paul N. Epstein[1]

Many diabetic patients suffer from a cardiomyopathy that cannot be explained by poor coronary perfusion. Reactive oxygen species (ROS) have been proposed to contribute to this cardiomyopathy. Consistent with this we found evidence for induction of the antioxidant genes for catalase in diabetic OVE26 hearts. To determine whether increased antioxidant protection could reduce diabetic cardiomyopathy, we assessed cardiac morphology and contractility, Ca^{2+} handling, malondialdehyde (MDA)-modified proteins, and ROS levels in individual cardiomyocytes isolated from control hearts, OVE26 diabetic hearts, and diabetic hearts overexpressing the antioxidant protein catalase. Diabetic hearts showed damaged mitochondria and myofibrils, reduced myocyte contractility, slowed intracellular Ca^{2+} decay, and increased MDA-modified proteins compared with control myocytes. Overexpressing catalase preserved normal cardiac morphology, prevented the contractile defects, and reduced MDA protein modification but did not reverse the slowed Ca^{2+} decay induced by diabetes. Additionally, high glucose promoted significantly increased generation of ROS in diabetic cardiomyocytes. Chronic overexpression of catalase or acute in vitro treatment with rotenone, an inhibitor of mitochondrial complex I, or thenoyltrifluoroacetone, an inhibitor of mitochondrial complex II, eliminated excess ROS production in diabetic cardiomyocytes. The structural damage to diabetic mitochondria and the efficacy of mitochondrial inhibitors in reducing ROS suggest that mitochondria are a source of oxidative damage in diabetic cardiomyocytes. We also found that catalase overexpression protected cardiomyocyte contractility in the agouti model of type 2 diabetes. These data show that both type 1 and type 2 diabetes induce damage at the level of individual myocytes, and that this damage occurs through mechanisms utilizing ROS. *Diabetes* 53: 1336–1343, 2004

From the [1]Department of Pediatrics, University of Louisville School of Medicine, Louisville, Kentucky; and the [2]Department of Anatomy and Cell Biology, University of North Dakota, Grand Forks, North Dakota.

Address correspondence and reprint requests to Paul N. Epstein, PhD, Department of Pediatrics, University of Louisville School of Medicine, 570 S. Preston St., Baxter Biomedical Building, Suite 304, Louisville, KY 40202. E-mail: paul.epstein@louisville.edu.

Received for publication 26 June 2003 and accepted in revised form 5 January 2004.

CM-H_2DCFDA, 5-(6)-chloromethyl-2′,7′-dichlorodihydrofluorescein diacetate; FFI, Fura 2 fluorescence intensity; GAPDH, glyceraldehyde 3-phosphate dehydrogenase; MDA, malondialdehyde; MT, metallothionein; ROS, reactive oxygen species.

Both type 1 and type 2 diabetes have been documented to lead to congestive heart failure, even in the absence of coronary artery disease (1). This implies that diabetes is detrimental to cardiomyocytes, independent of macrovascular complications. Results from chemically induced insulinopenic (2) and genetically predisposed insulin-resistant (3) rodent models (4) as well as human histological (5) and clinical observations (6) provide support for this concept of a specific diabetic cardiomyopathy.

Oxidative damage is widely considered to be a cause of diabetic complications (7,8), and signs of oxidative damage are found in diabetic patients. Recent proposals (9) suggest that overproduction of reactive oxygen species (ROS) may be the initiating event leading to long-term development of diabetic complications. ROS, such as the superoxide radical, the hydroxyl radical, and hydrogen peroxide, are continuously produced in most cells under physiological conditions, and their levels are regulated by a number of enzymes and physiological antioxidants. Enzymes that detoxify ROS include superoxide dismutase (SOD; which produces hydrogen peroxide by dismutation of superoxide) and glutathione peroxidase, and catalase (the two enzymes that detoxify hydrogen peroxide). When the production of ROS exceeds the capacity of the cell to detoxify them, oxidative stress develops that is harmful to the integrity of biological tissue. Results from human and animal studies show that there is an association between oxidative damage and diabetic cardiomyopathy.

Our laboratory previously demonstrated that the antioxidant protein metallothionein (MT) can prevent or markedly reduce diabetic cardiomyopathy (10,11). We interpreted those results to mean that oxidative stress was essential for the development of diabetic cardiomyopathy. However, MT, in addition to being a powerful antioxidant protein, has other actions, including the binding of heavy metal ions, reducing apoptosis (12), and modulating transcription (13). Those other actions may have been critical to the protection afforded by MT. To verify that reduction of oxidative stress, by itself, is sufficient for protection, we have now tested a classic antioxidant enzyme, catalase, against diabetic cardiomyopathy.

Our previous tests were performed with a model of type 1 diabetes. Type 2 diabetes carries additional risk factors, including insulin resistance, obesity, and dyslipidemia. Type 2 diabetes is a far more common problem, and it is a major risk factor for congestive heart failure. There are

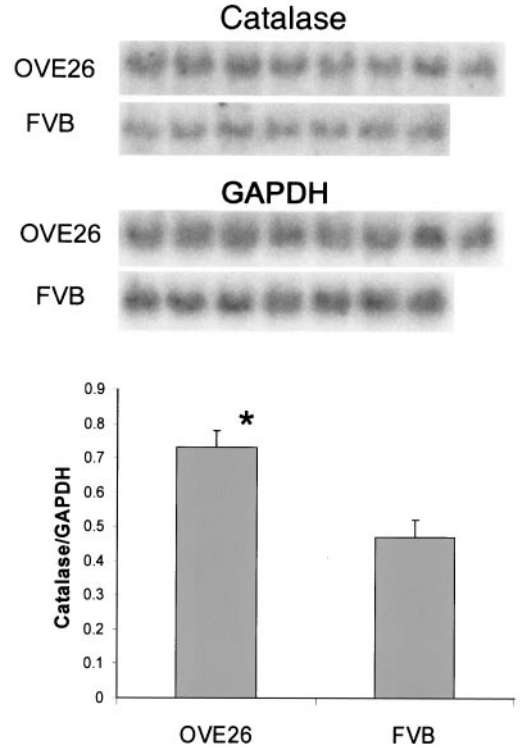

FIG. 1. Catalase RNA levels are increased in OVE26 hearts. Northern blots were prepared from total RNA of 5-month-old animals using eight OVE26 and seven FVB hearts. The lower graphs show the intensity of signals for catalase normalized to the intensity of the signal for GAPDH. *OVE26 is different from FVB by $P < 0.01$. Vertical bars indicate SE.

few studies of diabetic cardiomyopathy in animal models of type 2 diabetes (3,14), and those studies did not investigate the role of oxidative stress. Therefore, we tested whether catalase was protective in a recognized model of type 2 diabetes, the agouti (Ay) mouse.

RESEARCH DESIGN AND METHODS

OVE26 diabetic mice (15) and catalase transgenic mice that overexpress catalase 60-fold in the heart were previously described (16). Catalase and OVE26 mice were maintained on the inbred background FVB. OVE26-positive mice were identified by the presence of small eyes caused by the cointegration of the GR19 gene, which is expressed in the eye. Catalase-transgenic mice were identified by PCR of tail DNA. Mice positive for the OVE26 diabetes gene and the catalase transgene were designated OVE26C. Age-matched OVE26, OVE26C, and FVB mice of both sexes were obtained at 18–22 weeks of age.

Ay type 2 diabetic mice on the KK background were obtained from Jackson Laboratories. Catalase transgenic mice were bred to Ay mice. Offspring positive for the Ay gene were recognized by agouti coat color. Agouti-positive catalase-positive mice were designated AyC. All agouti experiments were performed on the F1 generation. These mice were designated FK for their 50% FVB and 50% KK genetic background. All type 1 and type 2 mating pairs used nondiabetic females to prevent the influence of diabetic gestation on cardiac phenotype. Mice were maintained on a 12-h light/dark cycle and received food (Purina Laboratory Rodent Diet 5001) and water ad libitum. The U.S. Department of Agriculture–certified institutional animal care committee approved all animal procedures.

RNA analysis. Northern blots were prepared and probed as previously described (17), using 10 μg of heart RNA from transgenic or control mice at 150 days of age. Oligonucleotide probes for mouse mRNAs for catalase and glyceraldehyde 3-phosphate dehydrogenase (GAPDH; GGAACATGTAGACCA TGTA-GTTGAGGTCAATGAAG) were labeled with [γ-^{32}P]ATP and polynucleotide kinase. The strength of the hybridization signal was determined on a Molecular Dynamics phosphoimager. Signals for catalase were normalized to the signals for GAPDH.

Western blot analysis of malondialdehyde. Hearts were frozen in liquid nitrogen, pulverized, and homogenized in 50 mmol/l sodium phosphate buffer (pH 7) containing 1 mmol/l EDTA, 40 μmol/l butylated hydroxytoluene, and protease inhibitor cocktail. The protein estimation was carried out using a Pierce BCA kit. Samples equivalent to 10 μg proteins were separated on 4–20% Tris-glycine gradient gels and transferred to polyvinylidene difluoride membrane. The membranes were blocked in 5% milk and incubated overnight in 1:2,000 dilution goat anti-malondialdehyde (MDA) polyclonal antibody from Academy Biomedical. The bands were visualized using peroxidase-conjugated affinity-purified donkey anti-goat IgG and an enhanced chemiluminescence detection system (Amersham). Signals for MDA were normalized to the signals for β-actin obtained from the same blot.

Electron microscopy. Procedures were carried out as previously described (17). Fixation was carried out by vascular perfusion through the left ventricle. The perfusates included washouts at 4°C of 35 ml half-strength Karnovsky's (18) fixative with 1% procaine, and 75 ml full-strength Karnovsky's final fix. Thin sections were observed in an Hitachi 7500 transmission electron microscope at initial magnifications of 4,000–15,000 diameters.

To quantify the morphologic features of cardiac tissues in each of the animal groups, transmission electron micrographs of randomly selected areas of left-ventricular thin sections were printed at identical magnifications. Two observers who were unaware of their origin rated these prints. Observers rated the morphology on a scale of 1–4 relative to a figure exhibiting near-perfect cardiac morphology. Figures were rated for overall morphology, which included the presence of edematous areas, myelin figures, and overall organization; mitochondrial morphology, which included mitochondrial packing, density, and shape; and myofibril morphology, which examined linearity of the Z lines and the linearity, regularity, and continuity of myofibrils.

Isolation of ventricular myocytes. Single ventricular myocytes were isolated by enzymatic dissociation with Liberase Blendzyme 4 (Roche Diagnostics, Indianapolis, IN) from adult mice by modification of described procedures (4). Briefly, animals were injected with heparin (1,000 units/kg i.p.) and anesthetized with ketamine (150 mg/kg i.p.) and xylazine (22.5 mg/kg i.p.). Their hearts were rapidly removed and perfused (at 37°C) with oxygenated (5% CO_2/95% O_2) Krebs-Henseleit calcium-free buffer (in mmol: NaCl 135, KCl 4.0, $MgCl_2$ 1.0, NaH_2PO_4 0.33, HEPES 10, glucose 10, and Butanedione 10, pH 7.4). Hearts were then perfused with the same Ca^{2+}-free Krebs-Henseleit buffer with collagenase II (0.9 mg/ml) for 15–20 min until the heart became flaccid. After perfusion, the left ventricle was removed, minced, and resuspended with the same Ca^{2+}-free Krebs-Henseleit buffer at room temperature. Extracellular Ca^{2+} was added incrementally back to 1.2 mmol/l. Isolated myocytes were maintained at room temperature in a serum-free medium consisting of medium 199 (Gibco) with Hanks' salts containing 25 mmol HEPES for further mechanical and fluorescent studies. Mechanical properties remained relatively stable in myocytes for 8–10 h in the serum-free medium. Cell yield was 50–70%. There was no notable difference of yield between normal FVB, FK, and diabetic mice. Myocytes with obvious sarcolemmal blebs or spontaneous contractions were not used. Only rod-shaped myocytes with clear edges were used for recording of mechanical properties, intracellular Ca^{2+} transients, and ROS fluorescent measurement.

Cell shortening/relengthening. Mechanical properties of ventricular myocytes were assessed using a video-based edge-detection system (IonOptix, Milton, MA) (4). The cells were field stimulated at a frequency of 1.0 Hz for 4 ms, using a pair of platinum wires that were placed on opposite sides of the dish chamber and connected to a MyoPacer Field Stimulator (IonOptix). The polarity of the stimulatory electrodes was reversed frequently to avoid possible buildup of electrolyte by-products. The myocytes being studied were displayed on the computer monitor using an IonOptix MyoCam camera, which rapidly scans the image area every 8.3 ms such that the amplitude and velocity of shortening/relengthening was recorded with good fidelity. Soft-edge software (IonOptix) was used to capture changes in cell length during shortening and relengthening. Cell shortening and relengthening were assessed using the following indexes: peak shortening, time to 90% peak shortening (TPS_{90}), time to 90% relengthening (TR_{90}), and maximal velocities of shortening and relengthening (±dL/dt).

Intracellular fluorescence measurement of Ca^{2+}. A separate cohort of myocytes was loaded with Fura 2-AM (1.0 μmol/l) for 30 min, and fluorescence measurements were recorded with a dual-excitation fluorescence photomultiplier system (Ionoptix). Myocytes were placed in a dish chamber on the stage of an Olympus IX-70 inverted microscope and imaged through a Fluor 100× oil objective. Cells were exposed to light emitted by a 75-W lamp and passed through either a 360- or a 380-nm filter (bandwidths were ±15 nm), while being stimulated to contract at 1.0 Hz. Fluorescence emissions were detected between 480 and 520 nm by a photomultiplier tube after first illuminating the cells at 360 nm for 0.5 s and then at 380 nm for the duration of the recording protocol (333-Hz sampling rate). The 360-nm excitation scan was repeated at the end of the protocol, and qualitative changes in intracellular Ca^{2+} concentration ($[Ca^{2+}]_i$) were inferred from the ratio. Intracellular

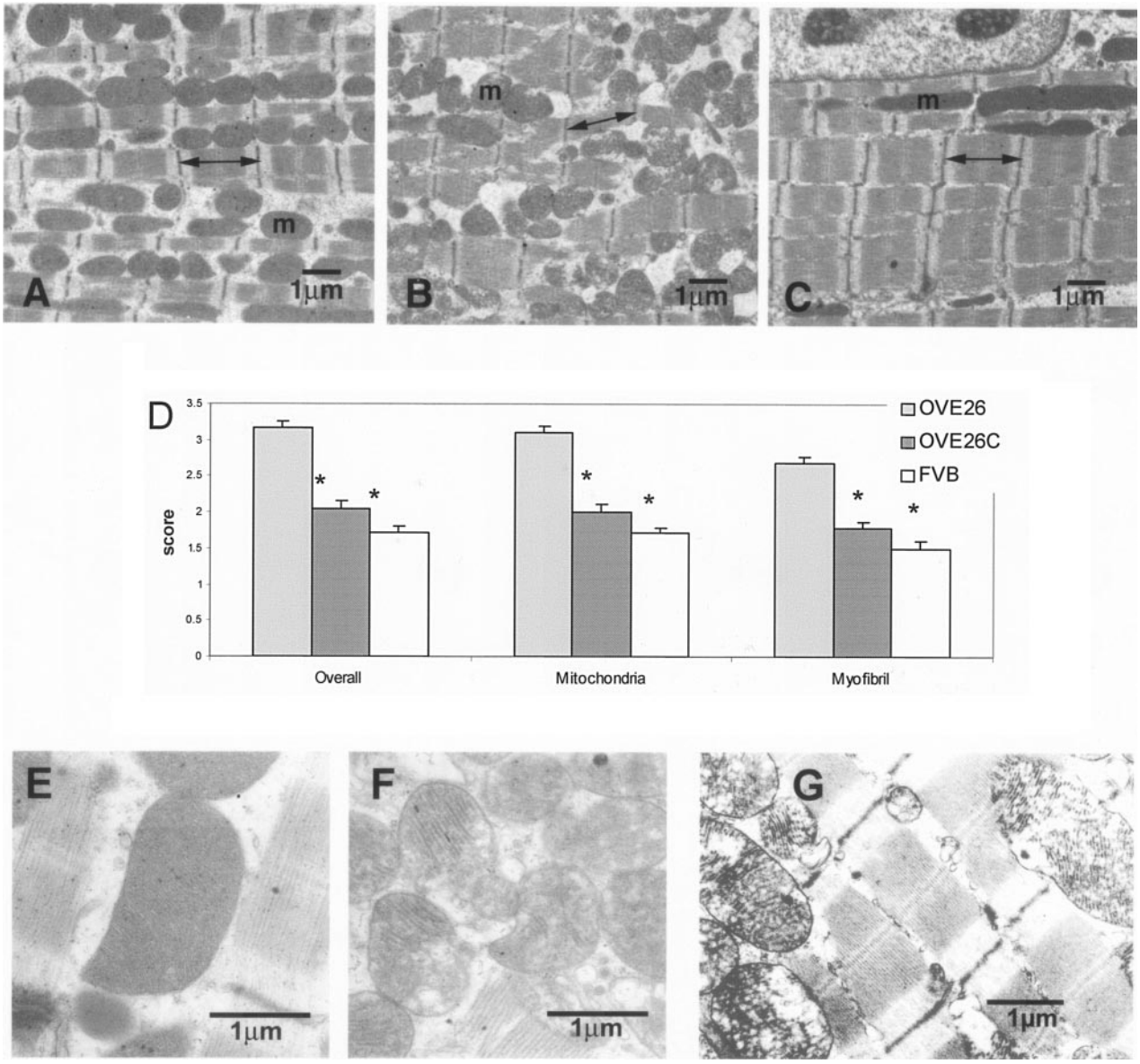

FIG. 2. Overexpression of catalase protects against morphologic damage. Electron micrographs of left ventricle in FVB (*A*), OVE26 (*B*), and OVE26C (*C*) mice at 5 months of age. *D*: Semiquantitative, blind, scoring of 32 randomly selected electron micrographs from each of two or three FVB, OVE26 diabetic, and OVE26C mice at 5 months. Higher magnification showing typical FVB mitochondria (*E*) and severely damaged OVE26 mitochondria (*F*). *G*: Portion of OVE26 left ventricle with normal myofibrils and damaged mitochondria. *OVE26 differs from OVE26C and FVB, $P < 0.001$.

Ca^{2+} transients were measured as changes in Fura 2 fluorescence intensity (FFI). ΔFFI was determined as the difference between the levels of Ca^{2+} in systolic and diastolic conditions (ΔFFI = peak FFI − baseline FFI). The time course of the fluorescence signal decay (τ: the duration where Ca^{2+} transient decays 67% from the peak level) was calculated to assess intracellular Ca^{2+} clearing rate.

Intracellular fluorescence measurement of ROS. The membrane-permeable probe 5-(6)-chloromethyl-2′,7′-dichlorodihydrofluorescein diacetate (CM-H_2DCFDA) enters cardiomyocytes and produces a fluorescent signal after intracellular oxidation by ROS such as hydrogen peroxide and hydroxyl radical (19). Intracellular oxidant stress was monitored by measuring changes in fluorescence resulting from intracellular probe oxidation. Isolated myocytes were loaded with 1 μmol/l CM-H_2DCFDA (Molecular Probes, Eugene, OR) for 30 min. The cardiomyocytes from each group were incubated at room temperature in M199 medium with normal glucose concentration (5.5 mmol/l) or high glucose (25 mmol/l). Myocytes were fixed in 4% paraformaldehyde after incubation and stored at 4°C for up to 16 h before imaging. Fluorescence intensity from individual cells was measured using an excitation wavelength of 485 nm and an emission wavelength of 530 nm. Cells were sampled at random in each preparation, using an Olympus IX70 inverted microscope equipped with a digital-cooled charge coupled device camera and ImagePro image analysis software (Media Cybernetics, Silver Spring, MD). Fluorescence was calibrated with InSpeck microspheres (Molecular Probes). Calibration curves were generated, and cell brightness was measured. The InSpeck microspheres were used as internal standards. After subtraction of background fluorescence, individual cell values were determined as the ratio of myocyte to standard bead fluorescence.

Data analysis. Data are expressed as the means ± SE. Statistical comparisons were performed by ANOVA and Bonferroni post hoc test among different groups. Significance was defined as $P < 0.05$.

RESULTS

Gene expression of antioxidant enzymes. Oxidatively stressed cells respond by induction of protective enzymes. In OVE26 hearts expression of catalase mRNA was increased by 40% compared with control hearts (Fig. 1). This was less induction than that reported for streptozotocin-induced (20,21) and alloxan-induced (22) diabetic models, but it was similar to results obtained with hearts from the

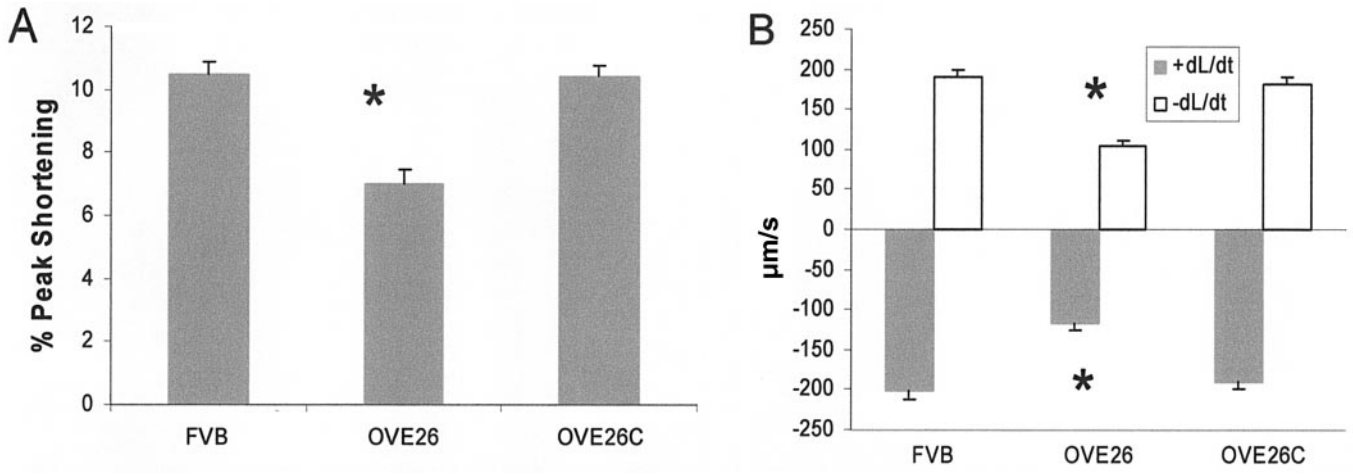

FIG. 3. The catalase transgene protects cardiomyocyte contractility. *A*: Percent peak shortening. *B*: Rates of contraction (+dL/dt) and relaxation (-dL/dt). *OVE26 is different from FVB and OVE26C, $P < 0.01$. Values are the means from ≥60 myocytes derived from at least five mice per group. The mean value obtained from at least five contractions was obtained each cardiomyocyte. Vertical bars indicate SE.

BB rat, an autoimmune model of type 1 diabetes, which exhibited a 52% increase in catalase (23). The moderate increase in expression of catalase suggests that the heart is responding to diabetes-induced oxidative stress.

Cardiac morphology. Transmission electron microscopy was carried out to determine whether the catalase transgene could reduce the damage to morphology in left ventricular tissue produced by diabetes (Fig. 2). Typical morphology of FVB, OVE26, and OVE26C hearts is shown in Figs. 2*A*–*C*. Consistent with our previous observations (10), heart tissue from diabetic OVE26 animals showed disorganization of normal architecture, myelin figures, damaged mitochondria, and disrupted myofibrils. To verify our impression that overexpression of catalase was effective in reducing morphologic damage, semiquantitative ratings were made of random electron micrographs by observers blind to the origin of the picture. These figures were judged for overall morphology, mitochondrial structure, and myofibrillar substructure, as described in RESEARCH DESIGN AND METHODS. The results of this analysis (Fig. 2*D*) confirmed that catalase overexpression provided significant protection from diabetes-induced damage on all parameters of cardiac morphology.

Observation at higher magnification revealed focal areas in OVE26 hearts with severely damaged mitochondria. This is most apparent when comparing high-magnification pictures of typical FVB mitochondria (Fig. 2*E*) and severely damaged OVE26 mitochondria (Fig. 2*F*). Similarly damaged mitochondria were never seen in control hearts and almost never seen in OVE26C hearts. In some micrographs (Fig. 2*G*), relatively healthy-looking myofibers were juxtaposed to severely damaged mitochondria. This suggests that mitochondria were especially sensitive to diabetes-induced damage.

Cardiomyocyte contractility. Diabetes significantly impaired contractility in isolated cardiomyocytes (Fig. 3). OVE26 diabetes produced at least a 30% reduction in percent shortening, rate of shortening, and rate of relengthening. Figure 3 shows that catalase overexpression in OVE26C mice completely prevented this effect: contractility in FVB and OVE26C myocytes was indistinguishable.

Intracellular Ca^{2+} transients. As shown in Fig. 4, recovery of the Ca^{2+} transient occurred more rapidly in control FVB cardiomyocytes than in OVE26 myocytes. The effect of the catalase transgene on the Ca^{2+} transient was small. Calcium recovery times in OVE26 and OVE26C myocytes were not significantly different, and both were significantly slower than that in FVB cardiomyocytes.

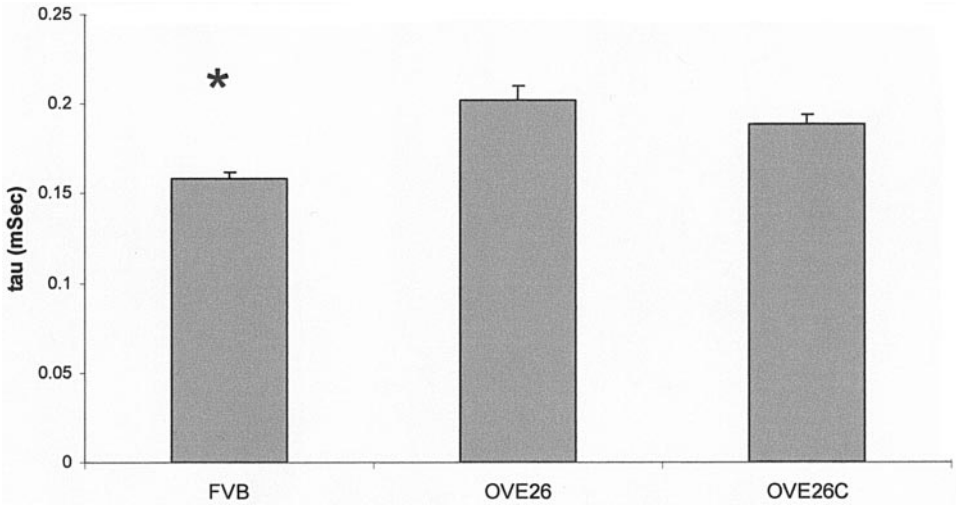

FIG. 4. Catalase does not prevent slower calcium reuptake in OVE26 myocytes. *Time required for calcium to return to 90% of baseline is longer in OVE26 and OVE26C myocytes, $P < 0.01$. Values are the means from ≥80 myocytes derived from four mice per group. The mean value obtained from at least five contractions was obtained for each cardiomyocyte. Vertical bars indicate SE.

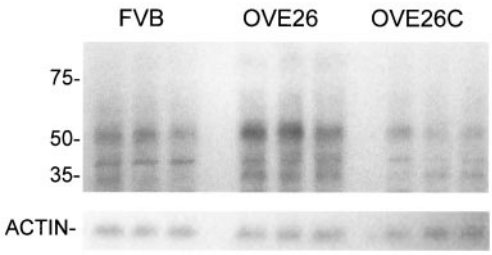

FIG. 5. Western blot of MDA-modified proteins in FVB control, OVE26 diabetic, and catalase-protected OVE26C diabetic hearts. The intensity of the 50-kDa protein on this blot was elevated 2.5-fold in OVE26 samples ($P < 0.02$) compared with FVB samples. The intensity of FVB and OVE26C immunostaining was not significantly different. MDA-modified proteins were recognized with polyclonal goat anti-MDA antibody and visualized with peroxidase-conjugated anti-goat antibody. Statistical analysis was performed by ANOVA and Tukey's post hoc test with three animals per group. Band intensities were normalized to β-actin intensity.

MDA-modified proteins. MDA is a by-product of lipid peroxides and thus an indicator for oxidative damage. Protein bands of ~35, ~50, and ~80 kDa gave increased signals with antibody to MDA in OVE26 hearts (Fig. 5). This effect was at least partially reversed by overexpression of catalase. The 50-kDa band, which was the most prominent MDA adduct, was quantified relative to β-actin staining and found to be increased by 2.5-fold in OVE26 hearts ($P < 0.02$) compared with FVB control hearts. The intensity of the 50-kDa band was not significantly different in FVB and OVE26C hearts.

Intracellular ROS levels$_2$. Figure 6 shows ROS production measured with CM-H_2DCFDA. Normal extracellular glucose produced similar ROS intensities among the cardiomyocytes from all three groups. Treatment of myocytes with high glucose (25 mmol/l) for 60 min did not affect the ROS level in control cardiomyocytes, but it caused a significant increase in the OVE26 cardiomyocytes. However, this effect of high glucose on ROS production was prevented by overexpression of catalase.

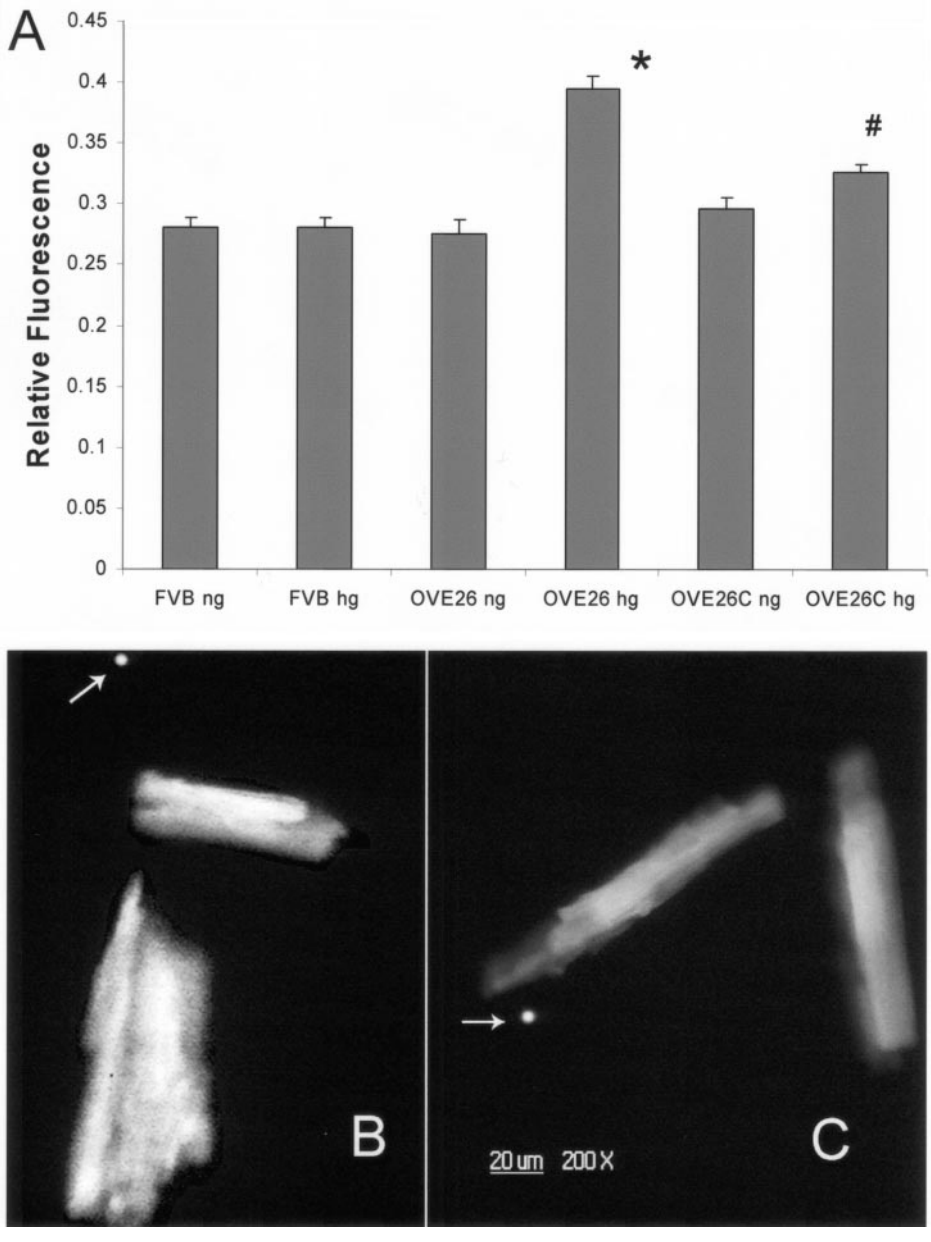

FIG. 6. Catalase reduces high-glucose–induced ROS production in diabetic myocytes. *A*: Isolated cardiomyocytes were exposed to normal glucose media (5.5 mmol/l) or high-glucose media (25 mmol/l) for 60 min, and ROS was measured by CM-H_2DCFDA fluorescence. *OVE26 exposed to high glucose was greater than all other groups ($P < 0.01$); #OVE26C was greater than all other groups except OVE26 exposed to high glucose and OVE26C exposed to normal glucose ($P < 0.05$). Vertical bars indicate SE. *B* and *C*: Typical fluorescence images of OVE26 myocytes exposed to high glucose (*B*) or low glucose (*C*). The arrows point to the fluorescence standardization bead used to normalize the intensity of all images. hg, high glucose; ng, normal glucose.

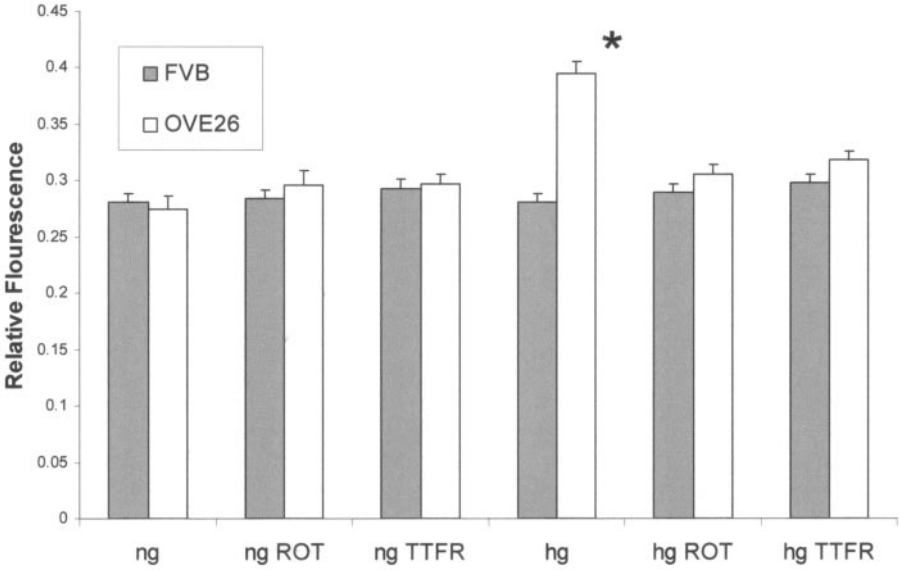

FIG. 7. Rotenone and thenoyltrifluoroacetone inhibit high-glucose–stimulated ROS production in diabetic OVE26 cardiomyocytes. *$P < 0.01$ vs. all other groups. Values are the means from 100 myocytes derived from four mice per group. Vertical bars indicate SE. hg, high glucose (25 mmol/l); ng, normal glucose (5.5 mmol/l); ROT, rotenone (5 μmol/l); TTFR, thenoyltrifluoroacetone (10 μmol/l).

Mitochondrial electron transport is an important source of superoxide anion. Inhibition of electron transport with rotenone or thenoyltrifluoroacetone eliminated the excess ROS production of OVE26 myocytes in high glucose (Fig. 7).

Cardiomyocyte contractility in type 2 diabetes. Catalase transgenic mice were bred to Ay diabetic mice to test whether catalase overexpression would be protective in this model of type 2 diabetes. Mice were analyzed at 130–145 days of age. F1 offspring that were Ay positive had significantly higher blood glucose levels than their Ay-negative siblings (266 ± 31 vs. 155 ± 13, $P < 0.05$). Ay-positive mice were also significantly more obese than their Ay-negative siblings (48 ± 0.9 vs. 36 + 2.5, $P < 0.01$). Ay diabetes significantly impaired cardiomyocyte contractility (Fig. 8), as indicated by reduced peak shortening and lower rates of shortening and relengthening. Overexpression of catalase provided almost complete protection against the reduction in contractility.

DISCUSSION

Our results show that catalase protects against diabetic cardiomyopathy. Nontransgenic diabetic hearts express 40% more mRNA from their endogenous catalase gene than control hearts. By increasing catalase activity 60-fold with a cardiac-specific transgene, we were able to significantly reduce the primary characteristics of diabetic cardiomyopathy. The transgene prevented morphologic damage to mitochondria and myofibrils. Impaired cardiomyocyte contractility was eliminated, and increased ROS production by high glucose was significantly reduced. Catalase was found to be effective in models of type 1 and type 2 diabetes.

The protection produced by catalase indicates that ROS are an essential intermediate in diabetic cardiomyopathy. This hypothesis was strengthened by the finding that several protein bands in diabetic hearts contained more MDA, a by-product of lipid peroxidation, than nondiabetic hearts. Catalase reversed the increase in MDA staining for the most prominent of these bands, confirming that catalase reduces diabetes-induced oxidative stress. Identification of the specific MDA-modified proteins may indicate which cardiac compartments are most stressed by diabetes and which proteins contribute to impaired myocyte function. In our previous (10,11) studies, we demonstrated that a transgene for the heavy metal–binding antioxidant

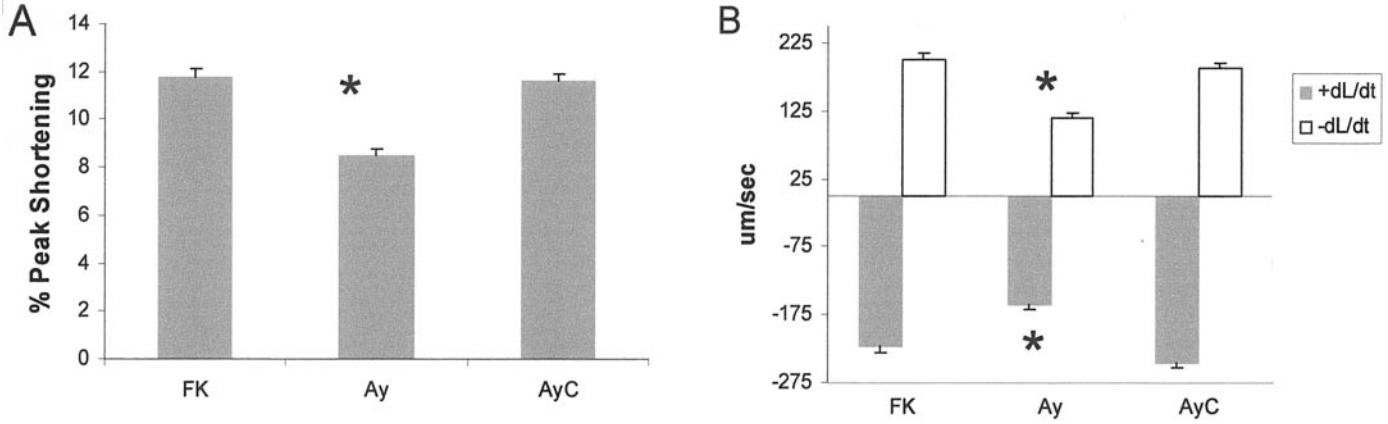

FIG. 8. The catalase transgene protects myocytes contractility in Ay diabetes. *A*: Percent peak shortening. *B*: Rates of contraction (+dL/dt) and relaxation (-dL/dt). *Ay diabetic myocytes are different from FK control and AyC myocytes, $P < 0.01$. Values are the means from ≥120 myocytes derived from five or six mice per group. Vertical bars are the SE.

protein MT was protective against diabetic cardiomyopathy. Unlike MT, which has several functions, catalase has only one major action in the cell: detoxification of hydrogen peroxide. Compared with MT, catalase was just as effective, except that it did not restore the normal rate of calcium reuptake. The additional protection by MT could be attributable to nonantioxidant actions of MT, or it could be a result of its broader range of antioxidant actions than catalase. MT can scavenge hydroxyl radical, superoxide, and peroxynitrite, whereas catalase is largely limited to hydrogen peroxide. One or more of the ROS that catalase cannot detoxify may therefore be involved in impaired calcium reuptake. On the other hand, these results show clearly that it is not essential to protect against all ROS in order to provide significant protection from diabetic cardiomyopathy. This should be of advantage in devising effective antioxidant therapies.

Our ROS measurement studies and morphology results implicate mitochondria as a major source of oxidative stress in OVE26 myocytes. Mitochondria are an obvious candidate because they are the major source of superoxide radical (24), they produce more ROS in a diabetic environment (9,25), and mitochondrial damage is commonly associated with cardiomyopathy (26) and diabetes (27). When diabetic myocytes were incubated in high glucose, they generated excess ROS compared with normal cardiomyocytes. This could be prevented by treatment with rotenone or thenoyltrifluoroacetone, inhibitors of electron transport from cytochromes I and II, respectively. If mitochondria are the major source of ROS, they should be exposed to the most oxidative stress and may suffer the most damage. Consistent with this, we observed in electron micrographs of OVE26 ventricles that mitochondria were the most obviously disrupted cellular component. If this damage impairs downstream mitochondrial electron transport complexes III (28) and IV (29), then the half-life of ubisemiquinone will be prolonged and ROS production increased. It is possible that diabetes produces initial damage to mitochondria, which increases ROS production, resulting in progressively greater damage to cardiomyocytes. If this scenario is correct, then catalase limits the damage diabetes inflicts on cardiomyocytes by providing protection from initial damage to mitochondria and/or protecting against enhanced mitochondrial ROS production.

The catalase transgene also protected cardiomyocytes of the agouti mouse. Diabetic pathology is very different in agouti and OVE26 models. Agouti mice are insulin resistant, obese, and moderately hyperglycemic. OVE26 mice are lean and severely hyperglycemic. OVE26 hearts are not insulin resistant, as judged by insulin-dependent phosphorylation of Akt (G.Y., N.S.M., R.V.D., S.X., M.X., E.C.C., P.N.E., unpublished results). Despite the differences, agouti diabetic cardiomyocytes showed deficits in contractility similar to OVE26 myocytes: percent contractility, rate of contractility, and rate of relaxation were all impaired. These results indicate that the insulin-resistant moderately hyperglycemic diabetes of agouti mice produces similar contractile impairment as insulinopenic, severely hyperglycemic diabetes of OVE26 mice. However, our preliminary results (not shown) suggest that calcium reuptake is either not impaired or much less impaired in agouti myocytes than in OVE26 myocytes. Catalase restored contractility to near-normal levels in agouti myocytes, as it did in OVE26 myocytes. The ability of a specific antioxidant protein to protect cardiomyocytes strongly implicates ROS as a mechanism of damage in type 2 diabetes. That both type 1 and 2 diabetes should act through ROS mechanisms is reasonable. Although there are many hypothesized mechanisms of increased ROS production in diabetes, all are initiated by hyperglycemia. Both the agouti and OVE26 models demonstrated hyperglycemia, albeit to a different extent. Because insulin resistance alone has been shown to impair cardiomyocyte function (30), it is likely that this added to the detrimental effects of the mild hyperglycemia in the agouti mouse. The fact that catalase was effective in agouti cardiomyocytes provides one of the first indications that ROS are an essential cause of diabetic cardiomyopathy in type 2 diabetes

ACKNOWLEDGMENTS

This work was supported by grants from the National Institutes of Health (HL62892, HL6677, and RR17702), the Commonwealth of Kentucky Research Challenge Trust Fund, and the University of Louisville Center for Genetics and Molecular Medicine.

We thank Donna Laturnus for technical assistance with electron microscopy.

REFERENCES

1. Jaffe AS, Spadaro JJ, Schechtman K, Roberts R, Geltman EM, Sobel BE: Increased congestive heart failure after myocardial infarction of modest extent in patients with diabetes mellitus. *Am Heart J* 108:31–37, 1984
2. Brown RA, Walsh MF, Ren J: Influence of gender and diabetes on vascular and myocardial contractile function. *Endocr Res* 27:399–408, 2001
3. Belke DD, Larsen TS, Gibbs EM, Severson DL: Altered metabolism causes cardiac dysfunction in perfused hearts from diabetic (db/db) mice. *Am J Physiol Endocrinol Metab* 279:E1104–E1113, 2000
4. Ren J, Sowers JR, Walsh MF, Brown RA: Reduced contractile response to insulin and IGF-I in ventricular myocytes from genetically obese Zucker rats. *Am J Physiol Heart Circ Physiol* 279:H1708–H1714, 2000
5. Fein FS: Diabetic cardiomyopathy (Review). *Diabetes Care* 13:1169–1179, 1990
6. Zarich SW, Nesto RW: Diabetic cardiomyopathy. *Am Heart J* 118:1000–1012, 1989
7. Marra G, Cotroneo P, Pitocco D, Manto A, Di Leo MA, Ruotolo V, Caputo S, Giardina B, Ghirlanda G, Santini SA: Early increase of oxidative stress and reduced antioxidant defenses in patients with uncomplicated type 1 diabetes: a case for gender difference. *Diabetes Care* 25:370–375, 2002
8. Penckofer S, Schwertz D, Florczak K: Oxidative stress and cardiovascular disease in type 2 diabetes: the role of antioxidants and pro-oxidants. *J Cardiovasc Nurs* 16:68–85, 2002
9. Nishikawa T, Edelstein D, Du XL, Yamagishi S, Matsumura T, Kaneda Y, Yorek MA, Beebe D, Oates PJ, Hammes HP, Giardino I, Brownlee M: Normalizing mitochondrial superoxide production blocks three pathways of hyperglycaemic damage. *Nature* 404:787–790, 2000
10. Liang Q, Carlson EC, Donthi RV, Kralik PM, Shen X, Epstein PN: Overexpression of metallothionein reduces diabetic cardiomyopathy. *Diabetes* 51:174–181, 2002
11. Ye G, Metreveli NS, Ren J, Epstein PN: Metallothionein prevents diabetes-induced deficits in cardiomyocytes by inhibiting reactive oxygen species production. *Diabetes* 52:777–783, 2003
12. Kang YJ, Zhou ZX, Wu H, Wang GW, Saari JT, Klein JB: Metallothionein inhibits myocardial apoptosis in copper-deficient mice: role of atrial natriuretic peptide. *Lab Invest* 80:745–757, 2000
13. DeMoor JM, Koropatnick DJ: Metals and cellular signaling in mammalian cells. *Cell Mol Biol* (*Noisy-le-grand*). 46:367–381, 2000
14. Belke DD, Betuing S, Tuttle MJ, Graveleau C, Young ME, Pham M, Zhang D, Cooksey RC, McClain DA, Litwin SE, Taegtmeyer H, Severson D, Kahn CR, Abel ED: Insulin signaling coordinately regulates cardiac size, metabolism, and contractile protein isoform expression. *J Clin Invest* 109:629–639, 2002

15. Epstein PN, Overbeek PA, Means AR: Calmodulin-induced early-onset diabetes in transgenic mice. *Cell* 58:1067–1073, 1989
16. Kang YJ, Chen Y, Yu A, Voss-McCowan M, Epstein PN: Overexpression of metallothionein in the heart of transgenic mice suppresses doxorubicin cardiotoxicity. *J Clin Invest* 100:1501–1506, 1997
17. Liang Q, Carlson EC, Borgerding AJ, Epstein PN: A transgenic model of acetaldehyde overproduction accelerates alcohol cardiomyopathy. *J Pharmacol Exp Ther* 291:766–772, 1999
18. Karnovsky MJ: A formaldehyde-glutaraldehyde fixative for high osmolality for use in electron microscopy. *J Cell Biol* 35:137A–138A, 1965
19. Kajstura J, Fiordaliso F, Andreoli AM, Li B, Chimenti S, Medow MS, Limana F, Nadal-Ginard B, Leri A, Anversa P: IGF-1 overexpression inhibits the development of diabetic cardiomyopathy and angiotensin II-mediated oxidative stress. *Diabetes* 50:1414–1424, 2001
20. Wohaieb SA, Godin DV: Alterations in free radical tissue-defense mechanisms in streptozocin-induced diabetes in rat: effects of insulin treatment. *Diabetes* 36:1014–1018, 1987
21. Nishio Y, Taki H, Hidaka H, Kashiwagi A: Altered NF-kB activity and oxidative stress-related gene expression in cardiovascular tissues of diabetic rats. *Diabetes* 46 (Suppl. 1):A206, 1997
22. Genet S, Kale RK, Baquer NZ: Alterations in antioxidant enzymes and oxidative damage in experimental diabetic rat tissues: effect of vanadate and fenugreek (*Trigonellafoenum graecum*). *Mol Cell Biochem* 236:7–12, 2002
23. Wohaieb SA, Godin DV: Alterations in tissue antioxidant systems in the spontaneously diabetic (BB Wistar) rat. *Can J Physiol Pharmacol* 65:2191–2195, 1987
24. Brand MD: Uncoupling to survive? The role of mitochondrial inefficiency in ageing. *Exp Gerontol* 35:811–820, 2000
25. Du X-L, Edelstein D, Brownlee M: Free fatty acids inhibit endothelial cell prostacyclin production and nitric oxide synthetase (eNOS) activity by inducing mitochondrial superoxide overproduction (Abstract). *Diabetes* 50 (Suppl. 2):A152, 2001
26. DiMauro S, Hirano M: Mitochondria and heart disease. *Curr Opin Cardiol* 13:190–197, 1998
27. Giacomelli F, Wiener J: Primary myocardial disease in the diabetic mouse: an ultrastructural study. *Lab Invest* 40:460–473, 1979
28. Lesnefsky EJ, Gudz TI, Migita CT, Ikeda-Saito M, Hassan MO, Turkaly PJ, Hoppel CL: Ischemic injury to mitochondrial electron transport in the aging heart: damage to the iron-sulfur protein subunit of electron transport complex III. *Arch Biochem Biophys* 385:117–128, 2001
29. Duranteau J, Chandel NS, Kulisz A, Shao Z, Schumacker PT: Intracellular signaling by reactive oxygen species during hypoxia in cardiomyocytes. *J Biol Chem* 273:11619–11624, 1998
30. Dutta K, Podolin DA, Davidson MB, Davidoff AJ: Cardiomyocyte dysfunction in sucrose-fed rats is associated with insulin resistance. *Diabetes* 50:1186–1192, 2001